- Technical Paper -

EXPERIMENTAL STUDY ON AXIAL BEHAVIOR OF CONCRETE COLUMNS REINFORCED BY SBPDN REBARS

Aixin ZHOU[*1], Yuping SUN[*2], Takashi TAKEUCHI[*3], Mian JIA[*4]

ABSTRACT

This paper presents the experimental results of the axial compressive behavior of concrete columns reinforced by SBPDN rebars. A total of eighteen columns (nine squares and nine circles) were tested under axial compression, with hoop spacing, number of longitudinal rebars, and concrete strength being the main variables. The test results are evaluated in terms of strength, strain ductility, and toughness index. The results indicate that comparing with the square columns, the circular columns have higher strength but with lower strain ductility and toughness index.

Keywords: UHS rebar, RC column, axial compression, rebar buckling, experiment

1. INTRODUCTION

Due to their superior physical and mechanical properties, high-strength (HS) and ultra-high-strength (UHS) steel rebars (with yield strength over 1000MPa) have been more and more widely adopted to the construction of high earthquake-resistant structures [1], and high resilient concrete columns [2] as well as walls [3]. The authors have experimentally verified that using SBPDN rebar, an UHS rebar with low bond strength, as longitudinal tensile and compressive reinforcement could assure sufficient drift-hardening capability to concrete columns and walls [2, 3]. Meanwhile, the previous study also indicated that the lateral resistance of concrete walls reinforced by SBPDN rebars tended to decrease due to crushing of concrete in compressive zone and local buckling of SNPDN bars at so large drift levels as 3.0% [3]. Therefore, to more accurately evaluate the drift-hardening capability of concrete walls with SBPDN rebars, information on the axial behavior of concrete columns (struts) reinforced by SBPDN rebars indispensable.

A large number of experimental investigations have been carried out to understand the mechanical behavior of the concrete columns reinforced by normal-strength steel rebars [4-6]. However, there are few, if any, studies on mechanical behavior of concrete columns reinforced by either UHS rebars or SBPDN rebars. With the aim of understanding more fundamental behavior of concrete columns reinforced by SBPDN rebars, eighteen concrete short columns, simulating the compressive edge zones of concrete wall, were fabricated and tested under axial compression. Based on the test results, the influences of hoop spacing, number of longitudinal rebars, and concrete strength grade on the load-carrying capacity, longitudinal rebar buckling, strain ductility, and toughness index were examined and discussed. The obtained results are expected to provide some insights into the design of concrete shear walls reinforced by SBPDN rebars.

2. EXPERIMENTAL PROGRAM

2.1 Test Specimens

A total of eighteen columns, including nine square columns and nine circular columns, are fabricated and tested in this study. All columns are in height of 360 mm, with a cross-section side length of 150 mm for the square columns and a diameter of 150 mm for the circular columns. Fig.1 shows the elevation views of the test specimens. The middle height regions of the columns are selected as the areas of interest to facilitate the investigation of buckling of longitudinal rebars. In the regions of concern, three different hoop intervals, i.e., 50 mm, 75 mm, and 100 mm, are considered. The hoop interval decreased to 25 mm to ensure the longitudinal rebars would buckle at the middle height regions of the columns. The end plates, which were anchored on the longitudinal rebars using the bolt nuts, were used to facilitate the forming of the reinforcement cage. Both the end plates and bolt nuts would not be taken off and would be covered after casting concrete. After the columns were made, two steel jackets with the height of 95 mm were also mounted at two ends of each column to provide additional constraint for the concrete outside the concerned regions. By doing so, the columns were expected to be damaged only in the mid-height regions.

Fig.2 shows four types of cross-sectional configurations and longitudinal rebar arrangements in view of A-A cut off. Type-A and Type-B are square sections that consist of 4 and 6 rebars, respectively.

*1 Ph.D. Student, Graduate School of Engineering, Kobe University, JCI Student Member
*2 Professor, Graduate School of Engineering, Kobe University, JCI Member
*3 Assistant Professor, Graduate School of Engineering, Kobe University, JCI Member
*4 M.S. Student, Graduate School of Engineering, Kobe University, JCI Student Member

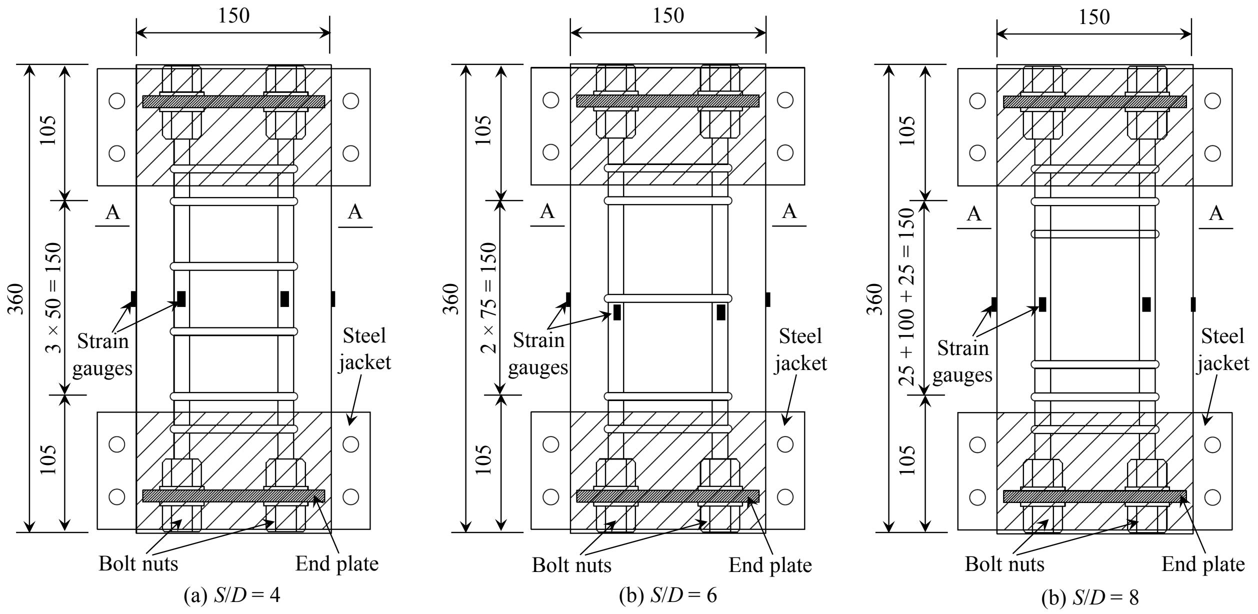

Fig.1 Elevation views of the test specimens (unit: mm)

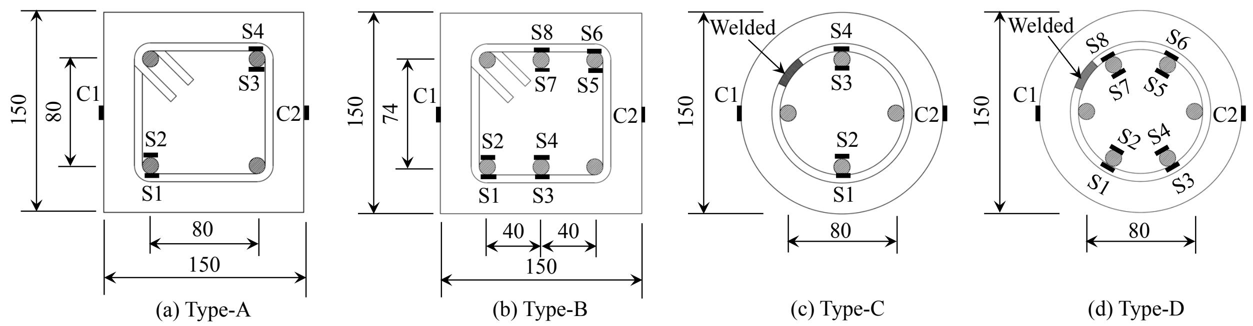

Fig.2 A-A cross-sections of the test specimens (unit: mm)

Type-C and Type-D are circular cross-sections that consist of 4 and 6 rebars, respectively. The summary of the test specimens is listed in Table 1.

2.2 Material Properties

In this study, SD295 steel rebar with a nominal diameter of 6.35 mm and SBPDN steel rebar with a nominal diameter of 12.6 mm are used as hoops and longitudinal rebars, respectively. Fig.3 shows the tensile stress-strain curves for both SD295 and SBPDN. All the mechanical specifications measured from three samples and the corresponding average values are listed in Table 2.

Two different grades of ready-mixed concrete made of Portland cement and coarse aggregates with the maximum particle size of 20 mm were used for constructing the columns. Based on the test results from three cylinders 100 × 200 mm in dimensions at 28 days after casting, the average values of compressive strength, splitting tensile strength, Young's modulus, and peak strain are 43.4 MPa, 3.2 MPa, 27.5 GPa, 0.0025 for the normal-strength grade concrete and 70.7 MPa, 6.1 MPa, 33.9 GPa, 0.0025 for the high-strength grade concrete.

2.3 Test Setup and Instrumentation

Axially monotonic compression load was

Table 1 Summary of the test specimens

No.	Type	D (mm)	d (mm)	S (mm)	S/D	f_{cc}' (MPa)
SA1	A	12.6	6.35	50	4	50.1
SA2	A	12.6	6.35	75	6	50.1
SA3	A	12.6	6.35	100	8	50.1
SB1	B	12.6	6.35	50	4	52.2
SB2	B	12.6	6.35	75	6	52.2
SB3	B	12.6	6.35	100	8	52.2
SC1	A	12.6	6.35	50	4	76.9
SC2	A	12.6	6.35	75	6	76.9
SC3	A	12.6	6.35	100	8	76.9
CA1	C	12.6	6.35	50	4	50.1
CA2	C	12.6	6.35	75	6	50.1
CA3	C	12.6	6.35	100	8	50.1
CB1	D	12.6	6.35	50	4	52.2
CB2	D	12.6	6.35	75	6	52.2
CB3	D	12.6	6.35	100	8	52.2
CC1	C	12.6	6.35	50	4	76.9
CC2	C	12.6	6.35	75	6	76.9
CC3	C	12.6	6.35	100	8	76.9

Note: D = diameter of longitudinal rebar; d = diameter of hoop rebar; S = hoop spacing; S/D = slenderness ratio; f_{cc}' = actual concrete compressive strength at the time of testing.

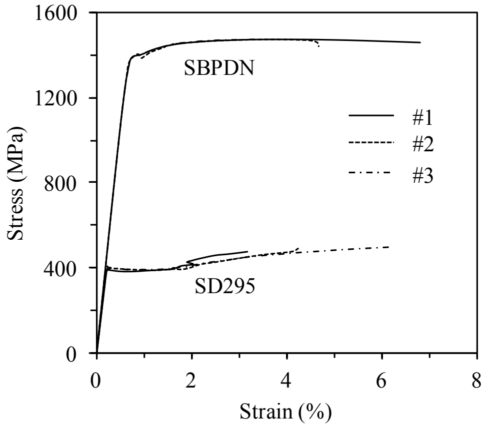

Fig.3 Tensile stress-strain curves of rebars

Table 2 Material properties of steel rebars

Grade	D (mm)	E_s (GPa)	f_y (MPa)	f_u (MPa)	ε_y (%)	ε_{sh} (%)
SD295	6.35	191	400	523	0.21	1.52
SBPDN	12.6	212	1397*	1470	0.86*	/

Note: D = diameter; E_s = Young's modulus; f_y = yield stress; f_u = tensile stress; ε_y = yield strain; ε_{sh} = strain at starting point of hardening branch; * based on the 0.2% offset method.

applied to the columns using a universal testing machine with a capacity of 2000 kN. Fig.4 shows the columns in the testing rig. As can be seen in the photograph, the upper steel plate was used to facilitate the installation of axial displacement measuring instruments, the lower steel plate was used to provide the same boundary conditions at the upper end. Both steel plates are in thick of 40 mm. Four linearly variable differential transformers (LVDTs), which were mounted at four corners of the steel plates, were used to measure the overall axial displacements. The axial strain of the column was measured by two axial strain gauges mounted at the concrete surface (see Fig.1). Two axial strain gauges were also placed on the opposite sides of the longitudinal rebar at mid-height section to measure the strain of the longitudinal rebars (see Fig.2). The lengths of the strain gauges for concrete and steel rebar were 30 mm and 2 mm, respectively. The tests were stopped when the axial shortening reached to 4% of the length of the specimen (i.e., average overall axial displacement of about 14.4 mm).

3. TEST RESULTS AND DISCUSSION

3.1 Axial Load-Displacement Curves

Fig.5 shows the axial load-displacement curves of all the tested columns. In these figures, the load was obtained from the load cell and the displacement was measured as the average value of four LVDTs (see Fig.4). As can be seen, the relationships of axial load and displacement are approximate linear at the initial stage. Then, owing to the appearance of cracks in cover concrete, the stiffness gradually decreases until the load

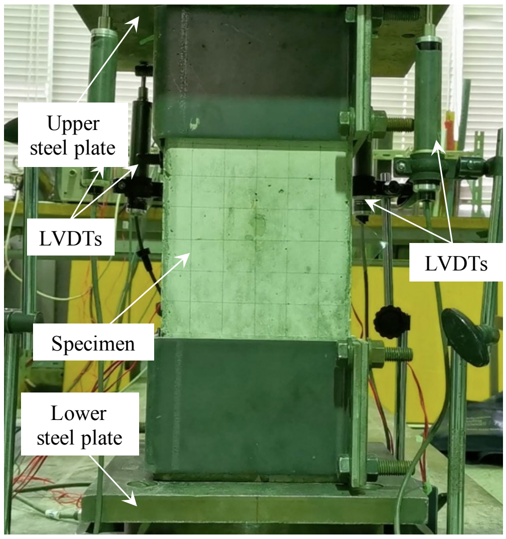

Fig.4 The column in the test rig

reaches the peak values. It is clearly shown that the peak load values increase with the decrease of hoop spacing. This is as expected because smaller S/D means the stronger lateral restraint for confined concrete, which results in a higher load-carrying capacity of the core concrete. Meanwhile, after the peak load points, the descending branch of the curves decreases at a faster speed in the specimen with larger S/D values, indicating the superior deformability of the columns with smaller hoop spacing. It should be noted that, for the circular columns with an S/D value of 4 and 6, the welded hoops suddenly fractured when the displacement reached about 7 ~ 8 mm (axial strain of about 2%). Which resulted in a significant drop for the load-carrying capacities. The main reasons for the fracture of welded hoops seemed to be the expansion of the core concrete and the buckling of the longitudinal rebars.

The peak loads (P_{max}), nominal peak stress (σ_{max}), strain at peak stress point (ε_{max}) are listed in Table 3. The strain and stress values are calculated using the loads and displacements based on the assumption that the strain and stress are uniformly distributed across the column cross-section. Fig.6 compares the nominal peak stresses for different columns. As can be seen, the circular columns (CA, CB, and CC groups) have higher nominal peak stresses than the square columns (SA, SB, and SC groups). In addition, the nominal peak stresses of both square and circular columns increase with the increase of number of longitudinal rebars and concrete strength grade.

The peak strain of the cover concrete (ε_c) was also recorded using the strain gauges mounted at the concrete surface. During the test, the concrete strains increased as the load increased. However, the concrete strains suddenly dropped after reaching the peak values, indicating the cover concrete was out of work. Thus, the concrete peak strain (ε_c) can be considered as the sign of the cover concrete spalling. The ε_c values determined from the average values of C1 and C2 strain gauges are listed in Table 3. As can be seen, there is no significant difference between the peak strains of

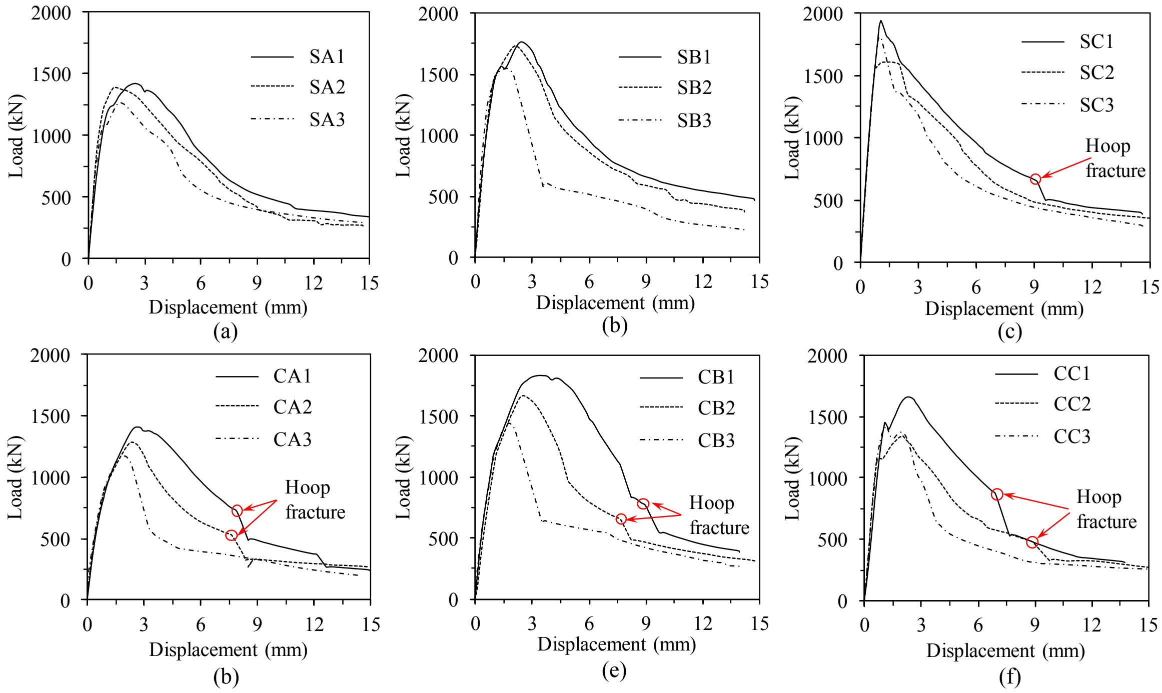

Fig.5 Axial load-displacement curves of different columns

Table 3 Summary of the compression test results

No.	P_{max} (kN)	σ_{max} (MPa)	ε_{max} (%)	ε_c (%)	$\frac{\varepsilon_c}{\varepsilon_{max}}$	Buckling strain, ε_b (%)				μ	I_{10}
						S1&S2	S3&S4	S5&S6	S7&S8		
SA1	1425	63.4	0.61	0.30	0.50	0.87	0.68	-	-	4.1	7.9
SA2	1396	62.0	0.39	0.23	0.59	0.30	0.77	-	-	4.2	8.1
SA3	1267	56.3	0.47	0.30	0.64	0.58	0.54	-	-	4.0	8.0
SB1	1770	78.7	0.67	0.35	0.51	0.40	0.67	0.39	0.60	3.0	7.0
SB2	1736	77.2	0.59	0.26	0.45	0.73	0.66	0.65	0.74	3.2	7.0
SB3	1549	68.9	0.46	0.28	0.62	0.29	0.27	0.46	0.45	3.1	6.6
SC1	1943	86.4	0.28	0.35	1.22	0.82	-	-	-	2.1	7.0
SC2	1605	71.3	0.33	0.26	0.80	0.86	0.22	-	-	2.5	7.2
SC3	1809	80.4	0.29	0.28	0.97	0.29	0.36	-	-	1.8	6.2
CA1	1408	79.7	0.72	0.27	0.38	0.71	0.71	-	-	2.7	6.3
CA2	1286	72.8	0.65	0.27	0.41	0.67	0.75	-	-	2.2	5.9
CA3	1170	66.2	0.53	0.31	0.57	0.58	0.26	-	-	2.2	5.2
CB1	1813	102.6	1.18	0.36	0.30	0.65	0.76	0.45	0.67	2.9	6.4
CB2	1672	94.6	0.71	0.23	0.33	0.89	0.62	0.66	0.70	2.2	5.4
CB3	1437	81.3	0.51	0.21	0.41	0.76	0.44	0.57	0.68	2.1	5.3
CC1	1661	94.0	0.65	0.36	0.55	0.77	0.79	-	-	3.1	7.3
CC2	1343	76.0	0.43	0.23	0.54	0.44	0.62	-	-	3.0	7.1
CC3	1429	80.9	0.33	0.33	1.00	0.26	0.26	-	-	2.9	6.5

the square and circular columns. The ε_c values range from 0.23% to 0.36%, along with a mean value of 0.29% and a standard deviation of 0.04%. In addition, except for SC1 and CC3, the ratios of ε_c to ε_{max} are all less than 1.0. This implies that the cover concrete does not contribute to the ultimate load-carrying capacity of RC columns.

3.2 Longitudinal Rebar Buckling

Fig.7 shows the tested columns after removing the damaged surrounding concrete. As expected, all the longitudinal bars buckled at the mid-height region of the columns. For the columns with a hoop spacing of 50 mm (S/D = 4), the longitudinal rebars buckled in the length of three intervals. For the specimens with a hoop spacing of 75 mm (S/D = 6), the longitudinal rebars buckled in the length of two intervals. For the specimens with a hoop spacing of 100 mm (S/D = 8), all the longitudinal rebars buckled in the length of one interval. It can be concluded that the buckling modes of longitudinal rebars are independent of the column cross-section shape, the concrete strength grade, and the number of longitudinal rebars.

Fig.8 illustrates the typical relationships of the

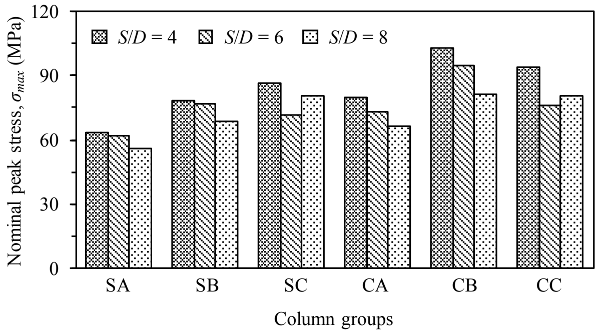

Fig.6 Comparison of nominal peak stress

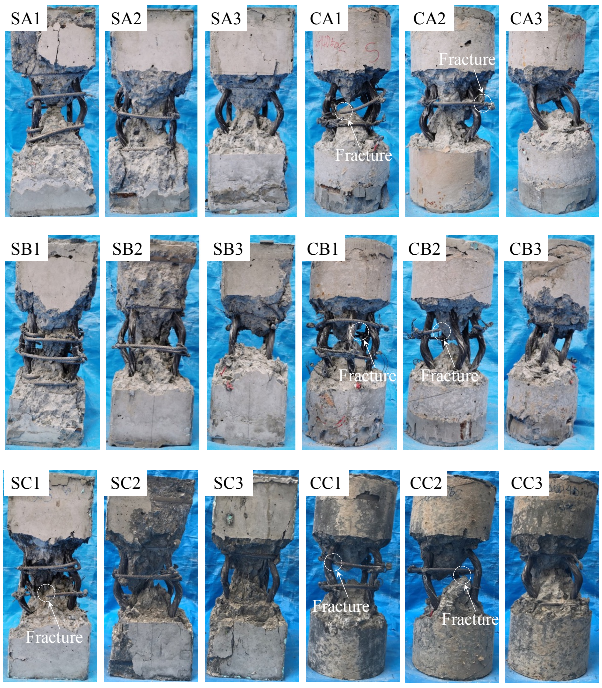

Fig.7 Buckled longitudinal rebars

measured strains and the average axial displacement for longitudinal rebars in the columns. The negative values of the ordinate represent the compression. It is clearly shown in Fig.8 that the strains measured from a pair of strain gauges mounted on the opposite sides of the longitudinal rebar were almost identical and increased linearly at the initial stage. As the axial displacement increased, however, the recorded axial strains began to deviate from each other. Due to the buckling induced bending stress in the longitudinal rebar, gauge S1 measured the strain of the section fiber subjected to a decrease in compression (convex side), and gauge S2 measured the strain of the section fiber subjected to an increase in compression (concave side). Following the criteria proposed by Rodriguez et al. [7], the onset of buckling was defined as the point where S2 – S1 value reached 20% of S1. The corresponding average strain value is referred to as the buckling strain (ε_b).

Table 3 lists the obtained buckling strains of the longitudinal rebars for all columns. As can be seen, the buckling strains range from 0.22% to 0.89%, and most of them below the yield strain of SBPDN rebars (ε_y = 0.86% as shown in Table 2). This implies that the longitudinal rebars buckled prematurely at the linear

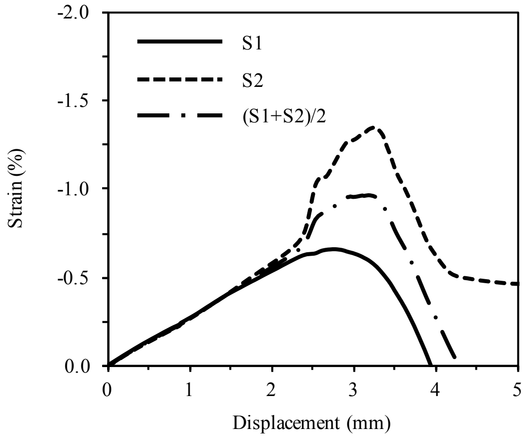

Fig.8 Typical strain-displacement curves of rebar

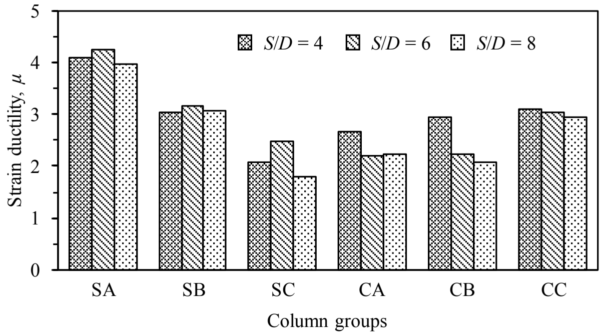

Fig.9 Comparison of strain ductility

elastic stage. The mean values of the buckling strains are 0.55% and 0.61% for the longitudinal rebars in square and circular columns, respectively. The main reason may be the higher rigidity of the welded hoops in the circular columns. In addition, the higher nominal peak stress (see Fig.7) of circular columns may be attributed to the higher buckling strains of the longitudinal rebars. Moreover, the mean values of the buckling strains are respectively 0.66%, 0.64%, and 0.44% for the longitudinal rebars in the columns with *S*/*D* values of 4, 6, and 8. It means that decreasing the hoop spacing is beneficial for increasing the buckling strains of longitudinal rebars.

3.3 Strain Ductility (μ)

Strain ductility (μ) is an important characteristic to reflect the deformability of RC columns under axial compression. It is often measured as the ratio of strain at 85% peak load of the descending branch to strain at the yield point [4]. The strain of yield point is measured by extending the line from the origin crossing to the 75% peak load [5]. The calculated strain ductility values of all columns are listed in Table 3 and the comparison results are indicated in Fig.9. In general, the ductility decreases with the increase of *S*/*D*. This is as expected because greater *S*/*D* means the weaker lateral restraint for confined concrete. The SA columns show the greatest strain ductility among all groups, indicating the optimal deformability of the columns fabricated with Type-A cross-section using the normal-strength grade concrete. For the square columns, increasing number of

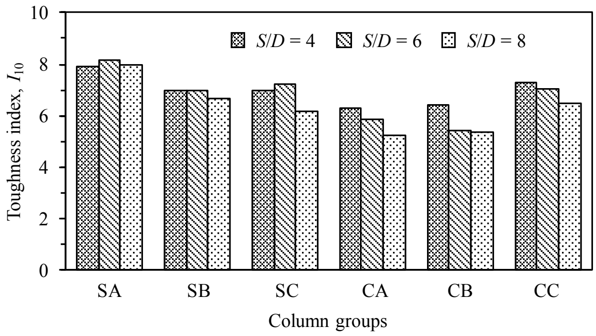

Fig.10 Comparison of toughness index

longitudinal rebars and concrete strength shows significant negative effects on the strain ductility. In contrast, for the circular columns, the reinforcement ratio has no effect on the strain ductility and the high-strength grade concrete significantly increases the strain ductility of the columns with higher *S*/*D* values.

3.4 Toughness index (I_{10})

The toughness index (I_{10}) measures the ability of energy absorption of the RC columns. It takes both strength and ductility into account and can be defined as the ratio of the total energy absorption to the pre-crack energy absorption [8]. The total energy absorption is determined from the area of the whole stress-strain curve, while the pre-crack energy absorption is determined from the area under the stress-strain curve up to the yield point. The yield point is the same to that defined in Section 3.3. The calculated toughness index values of all columns are listed in Table 3 and the comparison results are shown in Fig.10. Again, the SA columns exhibit the greatest toughness index among all groups. For the normal-strength grade concrete, regardless of the number of longitudinal rebars, it is obvious that the square columns (SA and SB groups) have superior energy absorption ability than the circular columns (CA and CB groups). However, for the high-strength grade concrete, the energy absorption abilities are comparable for square (SC group) and circular columns (CC group).

4. CONCLUSIONS

Based on the experimental results of eighteen RC columns reinforced by UHS rebar (with the tensile strength over 1400 MPa) under axial compression, the following conclusions can be drawn:

(1) Comparing the square columns, the circular columns have higher strength but with lower strain ductility and toughness index.
(2) The buckling modes of longitudinal rebars are independent of the column cross-section shape, the concrete strength grade, and the number of longitudinal rebars.
(3) The buckling strains of the longitudinal rebars indicate that the longitudinal rebars buckled prematurely at the linear elastic stage. Comparing with the square columns, the buckling strains are higher for the longitudinal rebars in the circular columns.
(4) The SA columns show the greatest strain ductility and toughness index among all groups, indicating the optimal deformability and energy absorption capacity of the columns fabricated with Type-A cross-section using the normal-strength grade concrete.

It should be noted that this work is limited to RC columns reinforced by UHS rebars, the comparison between the RC columns reinforced by normal-strength rebars should be conducted in further work.

ACKNOWLEDGEMENT

This work was partially supported by JSPS KAKENHI No. 19H02289. Neturen Co. Ltd is greatly appreciated for providing the SBPDN rebars.

REFERENCES

[1] Lepage A., Tavallali H., Pujol S., et. al. "Towards earthquake-resistant concrete structures with ultra-high strength steel reinforcement," 14th World Conference on Earthquake Engineering. Beijing, 2008.
[2] Sun Y., Cai G., Takeuchi T. "Seismic behavior and performance-based design of resilient concrete columns." International Journal of Applied Mechanics and Materials, Vol. 438, 2013, pp. 1453-1460.
[3] Fujitani T., Sun Y., Takeuchi T., et. al. "Study on effect of strength of rebars on the seismic performance of rectangular concrete walls," Japan Concrete Institute, Vol. 40(2), 2018, pp. 313-318.
[4] Duan L., Cooper T. "Displacement ductility capacity of reinforced concrete columns." Concrete International, Vol. 17(11), 1995, pp. 61-65.
[5] Samani A., Attard M., Foster S. "Ductility in concentrically loaded reinforced concrete columns." Australian Journal of Structural Engineering, Vol. 16(3), 2015, pp. 237-250.
[6] Razvi S., Saatcioglu M. "Strength and deformability of confined high-strength concrete columns." Structural Journal, Vol. 91(6), 1994, pp. 678-687.
[7] Rodriguez M., Botero J., Villa J. "Cyclic stress-strain behavior of reinforcing steel including effect of buckling." Journal of Structural Engineering, Vol. 125(6), 1999, pp. 605-612.
[8] Barr B., Liu K., Dowers R. "A toughness index to measure the energy absorption of fibre reinforced concrete." International Journal of Cement Composites and Lightweight Concrete, Vol. 4(4), 1982, pp. 221-227.